

## Special Pyrheliometer Shroud Development

E. Dennison  
Jet Propulsion Laboratory  
California Institute of Technology  
Pasadena, California 91109

Introduction The need for simple methods to compensate for circumsolar radiation became very important during the spring of 1982 when large amounts of dust appeared in the upper terrestrial atmosphere as a result of a volcanic eruption in Mexico. Prior to this time definitive calorimeter measurements at the JPL Parabolic Dish Site (PDTS) at the Edwards Test Station were limited to times when the insolation was greater than 950 W/sq.M, i.e., times when the amount of circumsolar radiation was negligible. This limitation was used because of the inconsistent data which was found at low elevation angles and on days of high circumsolar radiation.

After the appearance of the volcanic dust the maximum insolation was less than 900 W/sq.M and the amount of circumsolar radiation was significant. In addition, there was a very substantial increase in the presence of high thin cirrus clouds which added significant errors to the calorimeter measurements. The presence of circumsolar radiation is clearly shown in Figure 1. In this photograph of the PDC-1 concentrator the image of the sun is covered by the calorimeter and the bright halo around the calorimeter is the circumsolar radiation.

Insolation measurements are used to analyze atmospheric conditions, evaluate potential thermal power sites, and to determine the amount of input power to a power conversion unit. For the latter, the insolation measurements are used as an interpolation parameter between calorimeter measurements.

To insure that the insolation values accurately represent the input power to a power conversion unit it is important that the Field Of View (FOV) of the concentrator aperture and the insolation radiometer are

---

\*The work described in this paper was carried out or coordinated by the Jet Propulsion Laboratory, California Institute of Technology, and was sponsored by the U.S. Department of Energy through an agreement with the National Aeronautics and Space Administration.

the same. The word "radiometer" will be used to refer to both radiometers and pyrhemometers. If the calorimeter and the power conversion unit have the same aperture, the radiometer can be used to normalize all power measurements to a standard insolation value  $\times (1000 \text{ W/sq.M for the JPL data})$ .

This report covers the calculations, implementation, and results of the JPL use of this approach. Three instruments were used to measure the insolation: an Eppley Normal Incidence Radiometer (NIP) and two versions of the cavity radiometer developed by J. M. Kendall, Sr. at JPL. One of the Kendall radiometers was of the Mark VI windowless design used for calibration of radiometers and the other was the Mark III quartz window design used for routine field measurements. The shrouds used to limit the FOV of the radiometers were designed to simulate the FOV of the PDC-1 concentrator with the Cold Water Cavity Calorimeter (Figure 2).

Field of View Calculations The quantitative description of the FOV of a concentrator or radiometer will be referred to as the Angular Acceptance Function (AAF). The AAF is the fraction of the radiation coming from a point source at an infinite distance as a function of the angular distance of the point source from the optic axis of the concentrator or radiometer. The AAF does not depend on the angular size of sun but only on the geometric parameters of the concentrator or radiometer. The AAF will be 1.0 for a source on the optic axis and will decrease continuously from an inner limiting angle to zero at the outer limiting angle. The form of a concentrator AAF is different from the AAF of a radiometer because of the respective optical geometries. As a result, the radiometer AAF cannot be matched exactly to the concentrator AAF, but the differences between these functions can be made acceptably small.

Concentrator AAF One practical method for calculating the AAF of a solar concentrator was developed by Prof. G. F. Trentelman of Northern Michigan University using vector analysis. It has been found that in practice it is convenient to represent the AAF as a function of the ratio of the tangent of the source angle divided by the tangent of the receiver radius angle (receiver radius divided by the concentrator focal length). This parameter will be referred to as the "radius number." In this form the AAF changes substantially with the concentrator f-number (focal length divided by diameter) and insignificantly with receiver aperture. When the AAF is expressed in terms of these dimensionless parameters it can be easily applied to any paraboloidal concentrator with any receiver aperture (Figure 3). Slope errors cause some change in the AAF but in most cases these effects appear to be small.

Radiometer AAF The AAF of a radiometer can be calculated directly from the aperture and detector radii, the aperture/detector separation, and the angular distance of the point source from the optic axis. This calculation is based on the assumption that the detector aperture is uniformly sensitive. With the ratio of the front aperture to the

detector aperture and the tangent of the receiver aperture times the aperture/detector separation as free parameters the radiometer AAF can be calculated as a function of the radius number.

Matching Radiometer AAF to Concentrator AAF One practical method for finding the radiometer parameters which make the radiometer AAF fit the concentrator AAF is to use an interactive computer program. By a careful choice of parameters it is possible to make the radiometer AAF rapidly converge on the concentrator AAF. Because the concentrator AAF is determined from a finite number of rays, it can be fitted to a polynomial to give a smooth representation of the data. In practice this does not significantly change the radiometer parameters.

Experimental Results To verify the expected advantages of using a FOV limiting shroud on an insolation radiometer, a series of calorimeter measurements were made using the PDC-1 concentrator and the shrouded radiometers. One of the radiometers was an Eppley NIP mounted on the concentrator. The other radiometers were of the Kendall type and were attached to an equatorial mount with a clock drive. The boresight alignment images were checked frequently during the measurement period to insure that no erroneous data resulted from tracking errors.

The thermal power measured by the calorimeter and the insolation measured by the radiometers was plotted for each measurement period. To test the validity of this technique, the calorimeter values were divided by each of the radiometer values and the results were also plotted. These ratios gave the net power output of the concentrator normalized to 1000 W/sq.M under sky conditions which varied from light haze to thin cirrus clouds. No completely clear days occurred during the time these tests were made. There is no reason to believe that the normalized power values would differ from these values for completely clear skies. During the passage of the cirrus clouds the normalized power values showed a substantial variation over short periods of time as a result of long time constant of the calorimeter relative to the time constants of the radiometers.

Figures 4a and 5a show the radiometer data plots for two different days and Figures 4b and 5b show the corresponding plots of the direct and normalized power measurements. Figure 5b demonstrates that the normalized power is relatively constant under a wide range of sky conditions. The value of the normalized power in this figure was too high because of a faulty flow meter. This problem was corrected and the normalized power values shown in Figure 4b more accurately represent the performance of the PDC-1 concentrator.

The insolation values measured with these modified radiometers were lower than the values which would have been obtained with standard radiometers. However, the purpose of these measurements was to determine the relationship between the radiometers and the net power throughput

of the concentrator with a specific aperture. This calibration would have been used to determine the operating efficiency of the power conversion unit which was to have been used with this concentrator.

During this limited test program it was not possible to make a direct comparison between these shrouded radiometers and standard radiometers. However, this test program did demonstrate that the normalized power output of the PDC-1 concentrator was constant under a wide range of sky conditions.

Recommendations Because this program to evaluate the effectiveness of approach to insolation measurements was limited, it is recommended that these experiments be repeated with other concentrators and radiometers. These tests should be made with a wide range of sky conditions and solar elevation angles using both a standard and a shrouded NIP. These data would be very useful for determining the accuracy of existing NIP records. Finally, it is recommended that future site surveys be made with both standard and FOV limited NIP instruments to insure that proposed solar power systems are suitable for the proposed sites. This is most important when the proposed site has a substantial number of days with strong haze or thin clouds.

Conclusions This technique of matching the FOV of an insolation radiometer to the FOV of a specific concentrator and receiver aperture appears to be both practical and effective. It would appear that the efficiency of a power conversion unit will be too low if the insolation is measured with a radiometer which has a FOV which is larger than the FOV of the concentrator.

Author's Note An expanded version of this report with the AAF algorithms will be published at a later date.

Figure 1 PDC-1 with Cavity Calorimeter

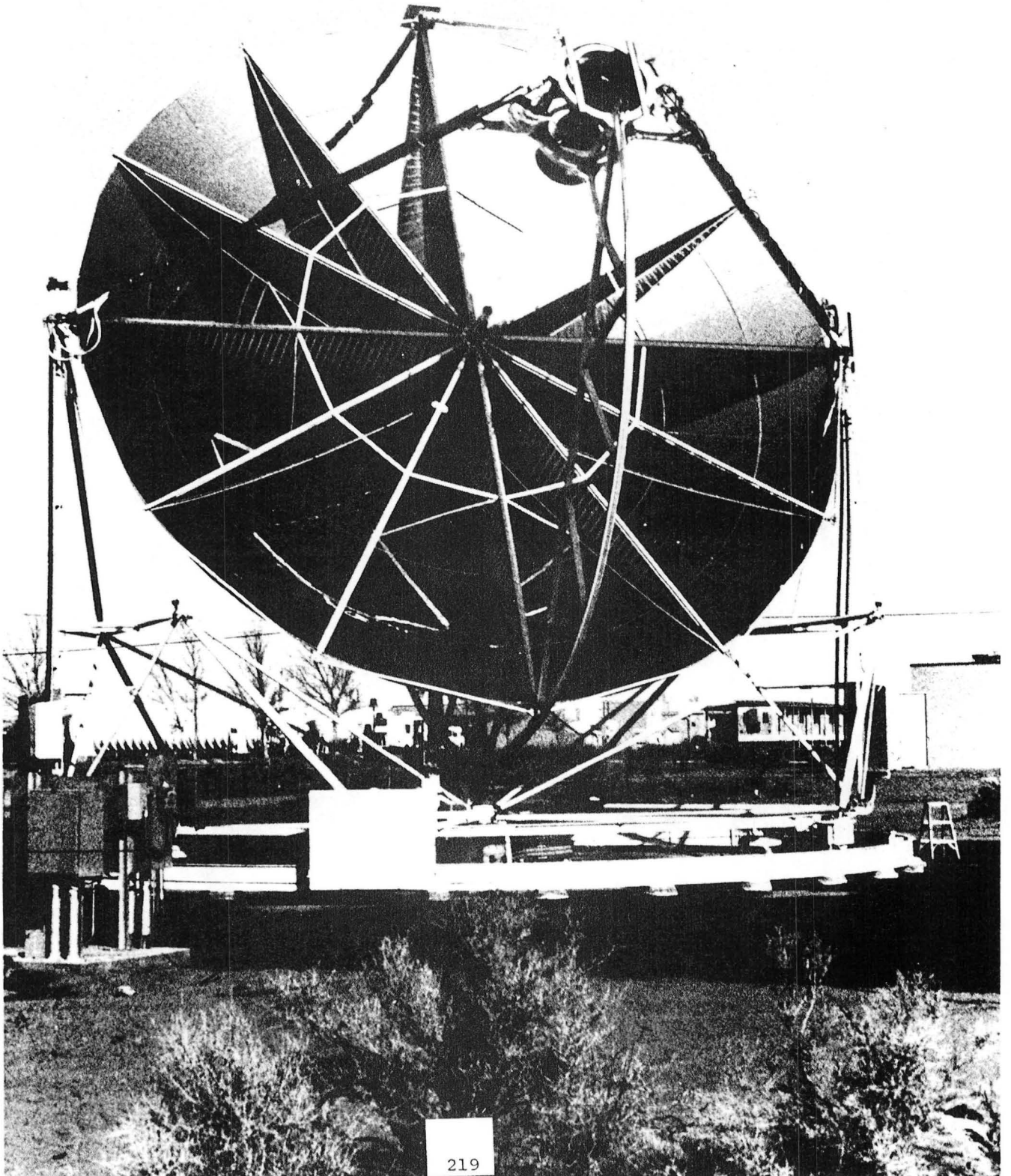
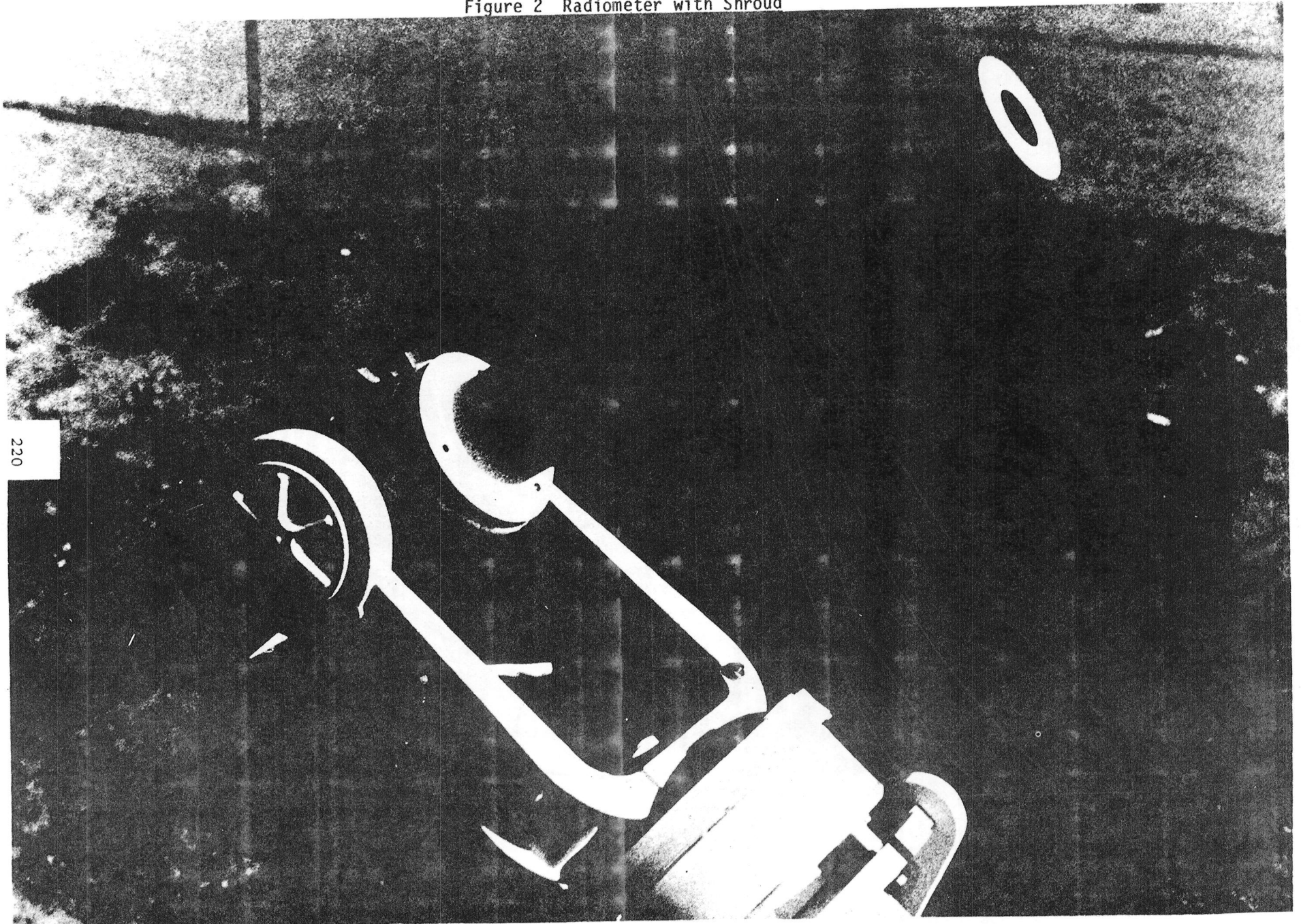


Figure 2 Radiometer with Shroud



220

Figure 3

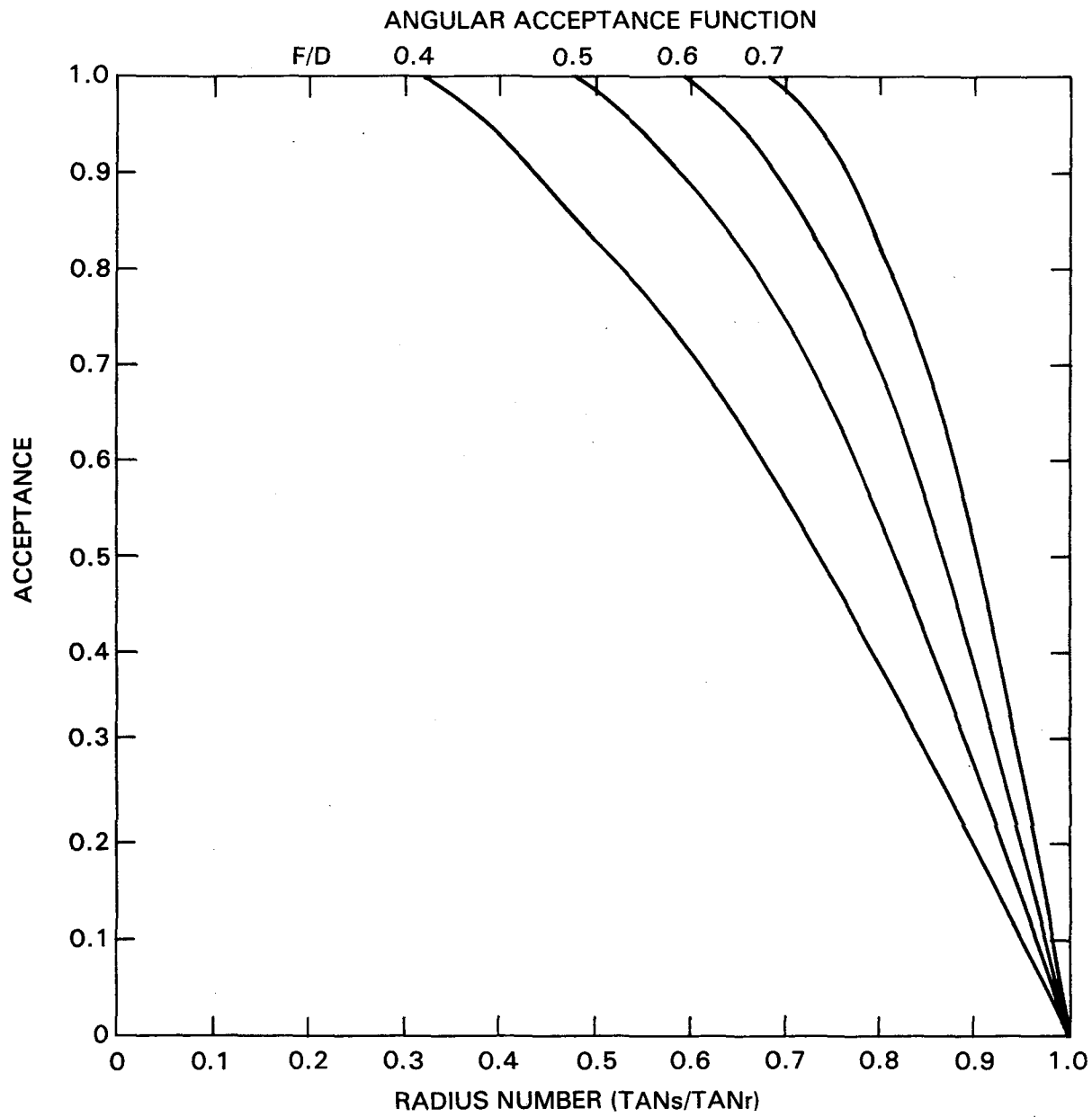


Figure 4a

PDC1: CWCC 100% MIRR.

TEST RUN: CWD192 14-JUL-83

1. EPPLEY DISH

N/M2 CHNL NO. 204

TIME INTERVAL BETWEEN SCANS: 30 SEC.

NUMBER OF SCANS: 194

2. KENDALL NIP

N/M2 CHNL NO. 203

3. KENDALL STD

N/M2 CHNL NO. 215

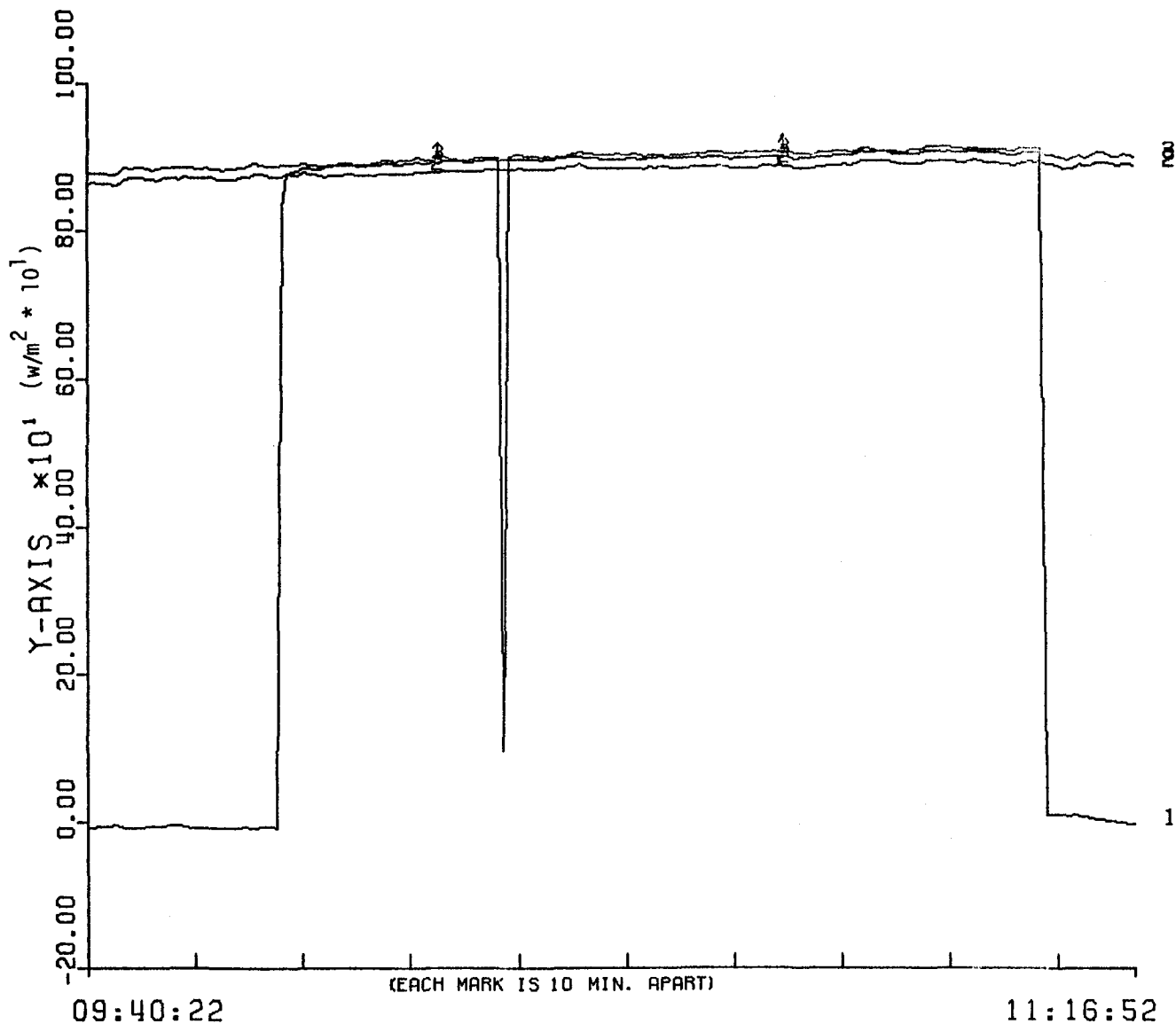


Figure 4b

PDC1; CWCC 100% MIRR.

TEST RUN: CW0192 14-JUL-83

TIME INTERVAL BETWEEN SCANS: 30 SEC.

NUMBER OF SCANS: 194

1. CORRECTD ENERGY

KWATTS CHNL NO. 502

2. COR. ENRGY (203)

KWATTS CHNL NO. 503

3. COR. ENRGY (215)

KWATTS CHNL NO. 504

4. EG OUTPUT ACTUAL

KWATTS CHNL NO. 501

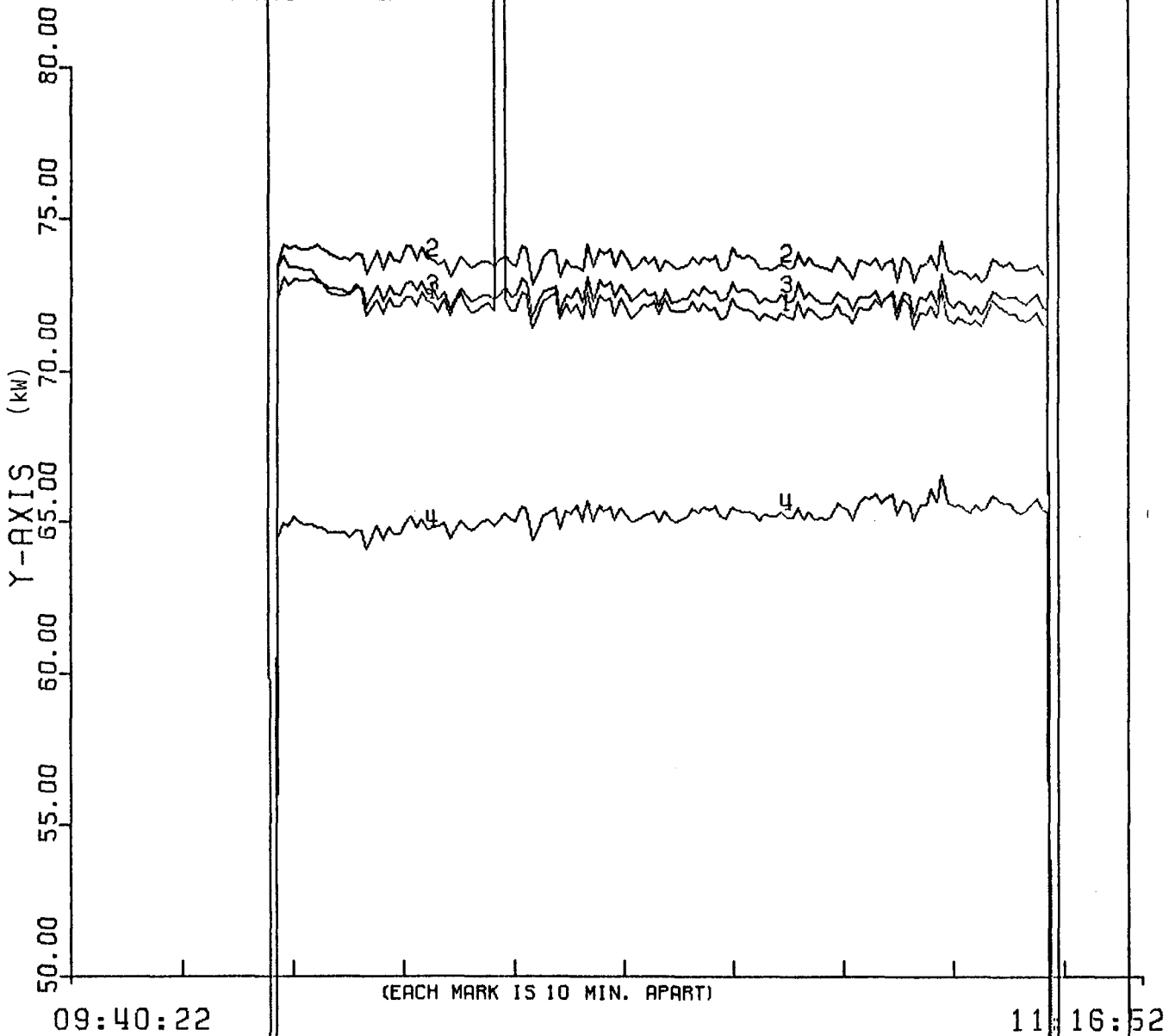


Figure 5a

PDC1: CWCC 100% MIRR.

TEST RUN: CW0178 22-FEB-83

1. EPPLEY DISH

W/M2 CHNL NO. 204

TIME INTERVAL BETWEEN SCANS: 30 SEC.

NUMBER OF SCANS: 642

2. KENDALL NIP

W/M2 CHNL NO. 203

3. KENDALL STD

W/M2 CHNL NO. 215

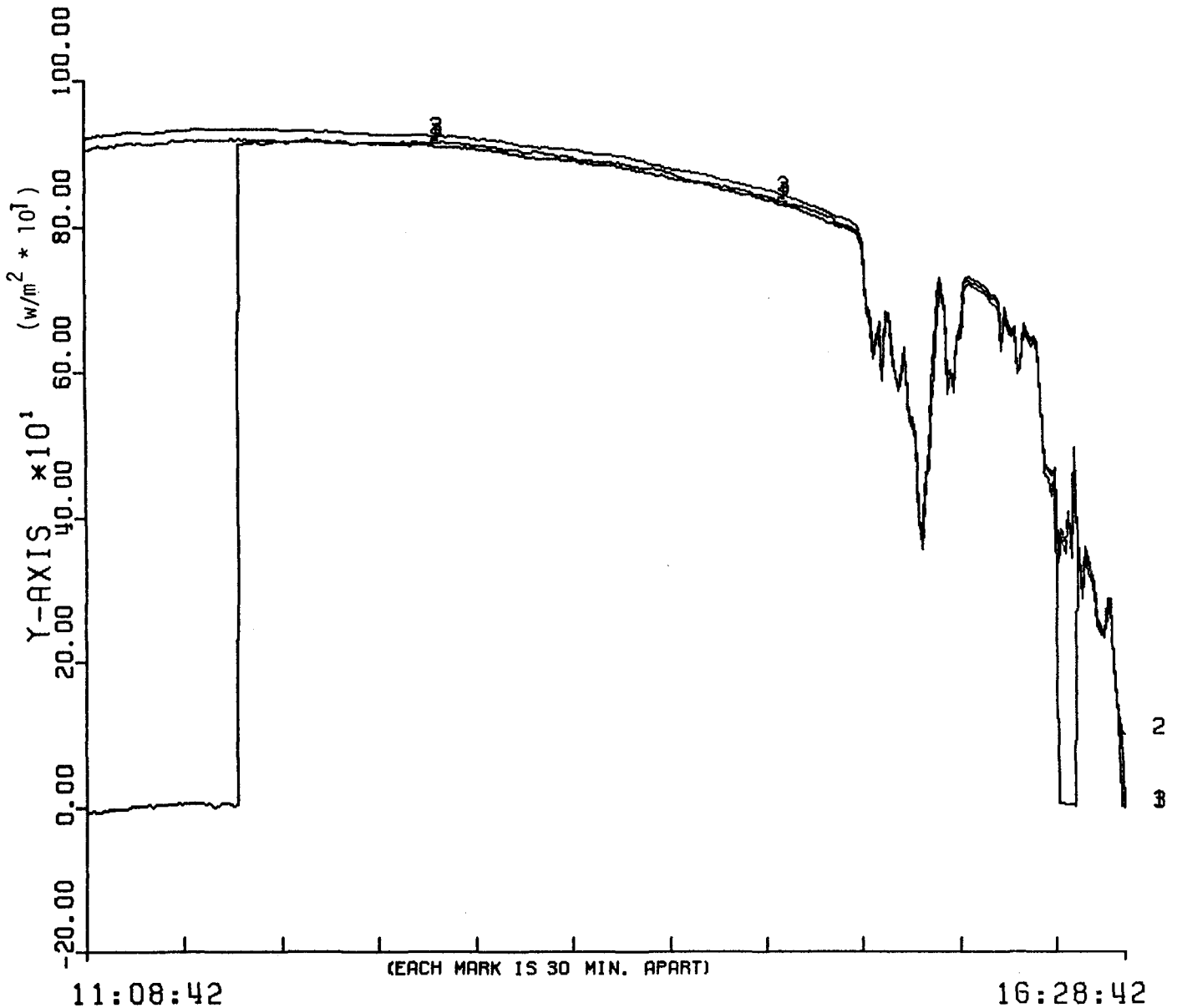


Figure 5b

POC1: CWCC 100% MIRR. FLOW CH. 213

TEST RUN: CW0178 22-FEB-83

1. EG OUTPUT ACTUAL

KWATTS CHNL NO. 501

TIME INTERVAL BETWEEN SCANS: 30 SEC

NUMBER OF SCANS: 642

2. CORRECTD ENERGY

KWATTS CHNL NO. 502

3. COR. ENRGY (203)

KWATTS CHNL NO. 503

4. COR. ENRGY (215)

KWATTS CHNL NO. 504

